THE JOURNAL OF PHYSICAL CHEMISTRY B

Article

pubs.acs.org/JPCB

Singlet−Singlet Exciton Recombination: Theoretical Insight into the Influence of High Density Regime of Excitons in Conjugated Polymers

Luiz Antonio Ribeiro Junior,* Wiliam Ferreira da Cunha, and Geraldo Magela e Silva*

Institute of Physics, Universidade de Brasília, 70.919-970 Brasilia, Brazil

ABSTRACT: Using a modified version of the Su−Schrieffer−Heeger (SSH) model combined with the extended Hubbard model (EHB), the recombination between a singlet exciton pair is investigated under the influence of an external electric field, electron−electron interactions, and temperature effects in the scope of a nonadiabatic evolution method. The excitons are positioned very close to each other in a way to mimic a high-density region in monomolecular conjugated polymer systems. Results show that there are mainly three possible channels resulting from singlet−singlet exciton recombination: (1) forming an excited negative polaron and an excited positive bipolaron, (2) forming two free and excited oppositely charged polarons, and (3) forming a biexciton. These results suggest that the recombination processes critically depends on the condition imposed to the system. The description of this dependence, as carried out in the present work, may provide guidance to improve the generation of free charge carriers in organic optoelectronic devices.

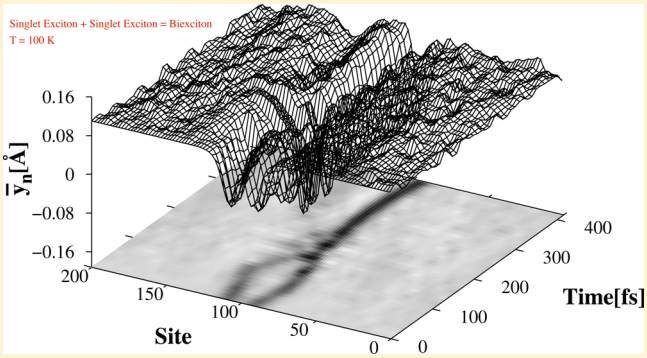

INTRODUCTION

Conjugated polymers have attracted considerable interest because the discovery of electroluminescence properties on phenyl-based organic semiconductors in the 90s. Their optoelectronic features combined with processing advantages, mechanical properties, and low cost make them attractive materials for the electronics industry to provide a promising new display technology. There are several potential applications such as organic photovoltaics devices (OPVs)[1−3] and polymer light emitting diodes (PLEDs).[4−6] In contrast to the conventional inorganic conductors, the fact that conjugated polymers are quasi-one-dimensional materials leads to the novel property of its lattice structure being easily distorted to form self-trapped elementary excitations. This can be accomplished either by charge injections or by a photoexcitation mechanism and results in the induction of self-localized electron states, such as an exciton.[7,8] In conjugate polymers, an exciton is a bound electron−hole pair state formed due to the strong electron−lattice interactions.[9] It is well-known that a large number of excitons are accumulated in working OPVs (forming a high-density excitons region) and have a significant probability of interacting and recombining. Also, the recombination of the excitons can occurs with other particles, for example, polarons and bipolarons.[10−12]

Among these excitations, the polaron and bipolaron acts on the system as charge carriers, whereas singlet exciton, the excited polaron, and biexciton are light emissive species.[13−15] It is suggested that the singlet−singlet exciton recombination possibly forms the above-mentioned particles and affects dramatically the working characteristics of OPVs. Although some possible mechanisms for recombination processes between excitons and charge carriers that considered electron−electron interactions and an external electric field have been proposed, no detailed theoretical investigations of how two singlet excitons recombine, when these effects are taken into account, have been reported. Furthermore, it has been generally accepted that temperature effects are one of fundamental importance on monomolecular recombination of mixed states composed of polarons and excitons.[16,17] Thus, the singlet−singlet exciton recombination in the presence of thermal effects is believed to be essential for OPVs devices. Understanding how the aforementioned effects acts on the monolayer exciton recombination process, which leads to free charge carriers generation, is crucial for the design of more efficient devices and requires a deeper phenomenological description.

In this paper, a systematic numerical investigation considering the influence of an external electric field, Coulomb interactions, and temperature effects on the singlet−singlet exciton recombination process is performed in a monolayer conjugated polymer system in terms of a nonadiabatic evolution method. The exciton pair recombination is investigated by considering a region in the conjugated polymer lattice with high-density of excitons. To mimic the high-density

Received: November 1, 2013
Revised: April 22, 2014
Published: April 22, 2014

dx.doi.org/10.1021/jp4107926 | J. Phys. Chem. B 2014, 118, 5250−5257

region, the excitons are positioned very close to each other. An Ehrenfest molecular dynamics is performed by using a one-dimensional tight-binding model including lattice relaxation. Combined with the EHM, an extended version of the SSH model is used to include external electric fields and Brazoviskii–Kirova symmetry breaking terms. Temperature effects are included by means of a canonical Langevin equation. The aim of this work is to give a physical picture of the products and their yields due to the recombination of a singlet–exciton pair in conjugated polymers, when electron–electron interactions, external electric field, and temperature effects are taken into account. The understanding of these important processes may provide guidance for improving the efficiency of free charge carriers generation in organic optoelectronic deveices.

MODEL AND METHOD

A conjugated polymer chain is used to study the influence temeperature effects on the generation os excited states. The Hamiltonian of the model is given by $H = H_{elec} + H_{latt} + H_{e-e}$.[18,19] The first term in eq 1 is the electronic part of the Hamiltonian modified to include an external electric field and the Brazovskii–Kirova symmetry-breaking and has the following form:

$$H_{elec} = -\sum_{n,s} (t_{n,n+1} C^{\dagger}_{n+1,s} C_{n,s} + hc) \tag{1}$$

were n indexes the sites of the chain. The operator $C^{\dagger}_{n,s}$ ($C_{n,s}$) creates (annihilates) a π-electron state at the nth site with spin s; K is the harmonic constant that describes a σ bond and M is the mass of a CH group. The parameter y_n is defined as $y_n \equiv u_{n+1} - u_n$ where u_n is the lattice displacement of an atom at the nth site. p_n is the conjugated momentum to u_n and $t_{n,n+1}$ is the hopping integral,[20] given by $t_{n,n+1} = e^{-i\gamma At}[(1 + (-1)^n \delta_0)t_0 - \alpha y_n]$, where t_0 is the hopping integral of a π-electron between nearest neighbor sites in the undimerized chain, α is the electron–phonon coupling, and δ_0 is the Brazovskii–Kirova symmetry-breaking term, which is used to take the cis-symmetry of the polymer into account. $\gamma \equiv ea/(\hbar c)$, with e being the absolute value of the electronic charge, a the lattice constant, and c the speed of light. The relation between the time-dependent vector potential $\mathbf{A}$ and the uniform electric field $\mathbf{E}$ is given by $\mathbf{E} = -(1/c)\dot{\mathbf{A}}$.[15] The second term in eq 1 is the Hamiltonian of the lattice backbone, which is treated classically:

$$H_{latt} = \sum_n \frac{K}{2} y_n^2 + \sum_n \frac{p_n^2}{2M} \tag{2}$$

where K is the harmonic constant that describes a σ bond and M is the mass of a CH group. The parameter y_n is defined as $y_n = u_{n+1} - u_n$ and p_n is the momentum conjugated to u_n.

The last contribution denotes e–e interactions and can be written as

$$H_{ee} = U \sum_i \left(C^{\dagger}_{i,\uparrow} C_{i,\uparrow} - \frac{1}{2}\right)\left(C^{\dagger}_{i,\downarrow} C_{i,\downarrow} - \frac{1}{2}\right) + V \sum_i (n_i - 1)(n_{i+1} - 1) \tag{3}$$

where U and V are the on-site and nearest-neighbor Coulomb repulsion strengths, respectively, and $n_i = C^{\dagger}_{i,\uparrow} C_{i,\uparrow} + C^{\dagger}_{i,\downarrow} C_{i,\downarrow}$.[21] It should be noted that the inclusion of the additional constant factors (related to the conventional description of the Hubbard model) is necessary to maintain the electron hole symmetry of the Hamiltonian. Several theoretical and experimental results have demonstrated that the primary excitation is the exciton, and electron–electron interactions are dominant over electron–lattice interactions in luminescent polymers.[22−27] Some theoretical studies that have considered the electron–lattice interactions also show that introduction of the lattice relaxation effect would not lead to an increase in binding energy of the exciton.[28,29] These facts enable us to handle electron–electron interactions in long chains and arrive at an understanding of electronic states in luminescent polymers without loss of essential physics. The parameters used here are $t_0 = 2.5$ eV, $M = 1349.14$ eV × fs^2/Å^2, $K = 21$ eV Å^{-2}, $\delta_0 = 0.05$, $\alpha = 4.1$ eV Å^{-1}, $a = 1.22$ Å, and a bare optical phonon energy $\hbar\omega_Q = \hbar(4K/M)^{(1/2)} = 0.16$ eV. These values have been used in previous simulations and are expected to be valid for conjugated polymers in general.[30−36]

To solve these equations numerically, first a stationary state that is self-consistent with all degrees of freedom of the system (the lattice plus electrons) is obtained. We begin by constructing the Hamiltonian from an arbitrary $\{y_n\}$ set of positions. By solving the time dependent Scrhödinger equation, we obtain a new set of coordinates $\{y'_n\}$. Iterative repetitions of this procedure yields a self-consistent initial state when $\{y_n\}$ is close enough to the solution. The equation of motion that describes the site displacement and provides the temporal evolution of the lattice is obtained by a classical approach. The nuclear dynamics is made with the Euler–Lagrange equations

$$\frac{d}{dt}\left(\frac{\partial \langle L\rangle}{\partial \dot{u}_n}\right) - \frac{\partial \langle L\rangle}{\partial u_n} = 0 \tag{4}$$

where $\langle L\rangle = \langle T\rangle - \langle V\rangle$. Equation 4 leads to an Newtonian equation $M\ddot{u}_n = F_n(t)$. Thus,

$$F_n(t) = M\ddot{u}_n = -K[2u_n(t) - u_{n+1}(t) - u_{n-1}(t)] + \alpha[B_{n,n+1} - B_{n-1,n} + B_{n+1,n} - B_{n,n-1}] \tag{5}$$

where $F_n(t)$ represents the force on the nth site.[37] Here, $B_{n,n'} = \sum'_{k,s} \psi^*_{k,s}(n,t)\, \psi_{k,s}(n',t)$ is the term that couples the electronic and lattice solutions. The primed summation represents a sum over the occupied states.

The total time dependent wave function was constructed by means of a combination of instantaneous eigenstates of the electronic Hamiltonian. The solutions of the time-dependent Scrhödinger equation can be put in the form

$$\psi_{k,s}(n,t_{j+1}) = \sum_l [\sum_m \varphi^*_{l,s}(m,t_j)\, \psi_{k,s}(m,t_j)] \times e^{(-i\varepsilon_l \Delta t/\hbar)} \varphi_{l,s}(n,t_j) \tag{6}$$

$\{\phi_l(n)\}$ and $\{\varepsilon_l\}$ are the eigenfunctions and the eigenvalues of the electronic part for the Hamiltonian at a given time t_j.[38] Equation 5, which governs the evolution of system, may be numerically integrated using the method $u_n(t_{j+1}) = u_n(t_j) + \dot{u}_n(t_j)\Delta t$ and $\dot{u}_n(t_{j+1}) = \dot{u}_n(t_j) + (F_n(t_j)/M)\Delta t$. Hence, the electronic wave functions and the lattice displacements at the $(j + 1)$th time step are obtained from the jth time step. At time t_j the wave functions $\{\psi_{k,s}(i,t_j)\}$ can be expressed as a series expansion of the eigenfunctions $\{\phi_{l,s}\}$ at that moment: $\psi_{k,s}(i,t_j) = \sum_{l=1}^{N} C^S_{l,k} \phi_{l,s}(i)$, where $C^S_{l,k}$ are the expansion coefficients. The occupation number for eigenstate $\phi_{l,s}$ is $\eta_{l,s}(t_j) = \sum'_k |C^S_{l,k}(t_j)|^2$.

dx.doi.org/10.1021/jp4107926 | J. Phys. Chem. B 2014, 118, 5250−5257

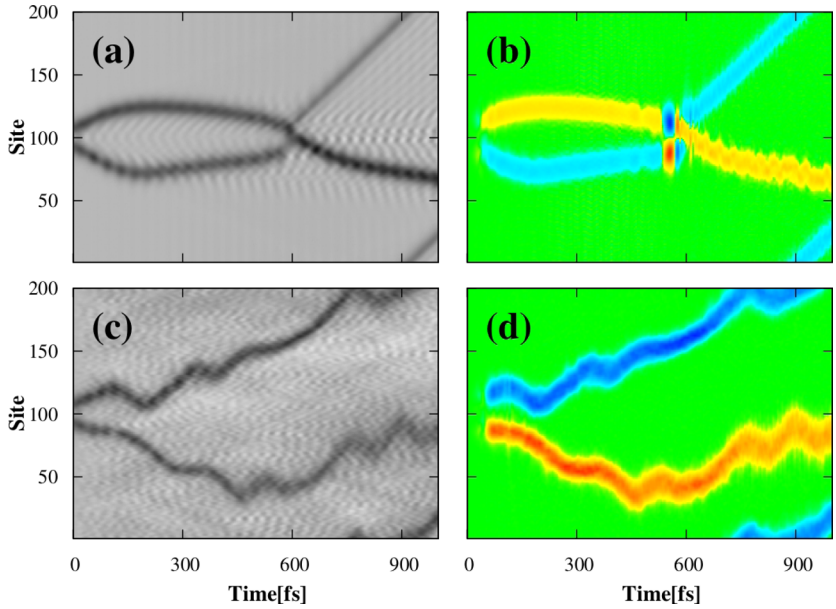

Figure 1. (a) Bond-length time evolution and (b) charge density time evolution for the channel 1 where E = 1.5 mV/Å, U = 0.3 eV, and T = 0 K. (c) Bond-length time evolution and (d) charge density time evolution for the channel 2 using E = 1.5 mV/Å, U = 0.2 eV, and T = 150 K.

$\eta_{l,s}(t_j)$ contains information concerning the redistribution of electrons among the energy levels.[39,40] Because our model assumes a classical treatment for the lattice, it is possible to use the Langevin approach to consider the thermal effects. It is settled a white stochastic signal $\zeta(t)$ as the fluctuation term, i.e., a signal with the following properties: $\langle\zeta(t) \equiv 0\rangle$ and $\langle\zeta(t)\ \zeta(t') = \Lambda\delta(t-t')\rangle$. A Stokes-like dissipation term is also included in this formalism. Therefore, eq 5 is modified to $M\ddot{u} = -\gamma\dot{u} + \zeta(t) + F_n(t)$. The relationship between ζ, γ, and the temperature T is given the fluctuation−dissipation theorem, $\Lambda = 2k_BT\gamma M$. It is important advise that this approach of considering thermal effects in conjugated polymers has ben used before in the literature and has good track record.[16,17,41−45]

RESULTS AND DISCUSSION

A systematic numerical investigation considering the influence of external electric field, Coulomb interactions, and temperature effects over the singlet−singlet exciton recombination dynamics is performed in systems composed of 200-site cis-polyacetylene with periodic boundary conditions. For the electric field, turned on quasi-adiabatically until 50 fs,[41] the values used in the simulations varied from 0.5 to 2.5 mV/Å with an increment of 0.5 mV/Å, whereas the on-site electron−electron interactions values considered are 0.1, 0.2, 0.3, 0.4, and 0.5 eV. The nearest-neighbor Coulomb repulsion strength was defined using the relation $V = U/2$. As already mentioned, the temperature is introduced by means of a Langevin equation to simulate the sites random motion. Thus, the measure of temperature is obtained through the classical equivalence $k_BT = M\dot{u}_n^2$. It is important to note, however, that special care must be taken on relating a given temperature value to a simulation at different times because the process of thermalization is not carried out instantaneously. In a previous work it was shown that the higher the desired temperature, the more time it takes for the system to relax into this regime.[41] Because one of the objectives is to perform a qualitative investigation on the temperature influence over the exciton pair recombination, we used 1000 fs for the time of simulation to carry out the analysis and guarantee that the lattice reaches up all the simulated temperature regimes.

Furthermore, the analysis of the quasi-particles dynamics is performed by considering the mean charge density $\overline{\rho}_n(t)$, derived from the charge density $\rho_n(t) = \sum'_{k,s}\psi^*_{k,s}(n,t)\ \psi_{k,s}(n,t)$, and the mean order parameter $\overline{y}_n(t)$. The expressions for these quantities are given by $\overline{\rho}(t) = 1 - [\rho_{n-1}(t) + 2\rho_n(t) + \rho_{n+1}(t)]/4$ and $\overline{y}(t) = (-1)^n[y_{n-1}(t) + 2y_n(t) + y_{n+1}(t)]/4$. The goal is to provide a better visualization of the simulations and consequently to perform a more accurate analysis of the results.

In this context, Figure 1 depicts the dynamical process of free charge carrier generation via singlet−singlet exciton recombination. The first channel reported here for the recombination mechanism is showed through the order parameter in Figure 1a and through the charge density time evolution in Figure 1b. For this case, the electric field strength and Coulomb interactions considered are 1.5 mV/Å and 0.3 eV, respectively, in the absence of temperature effects. Initially, the excitons are positioned very close to each other in a way to mimic a high-density region, as can be seen in the bond-length time evolution shown in Figure 1a. In conjugated polymers, the clearest difference between the triplet and singlet excitons is that the triplet states are more localized than singlet ones. In addition, the distortion at the center of the singlet state is shallower than the triplet state, and the dimerization pattern is also different between them.[46] A singlet exciton (SE) causes a distortion in the lattice of approximately 40 sites around its center. Considering this fact, to mimic a high-density region, the exciton pair is positioned within 70 sites of the lattice. The presence of such close pair of singlet excitons causes a considerable overlap of their wave functions. The above-mentioned differences between singlet and triplet states indicate that the exciton pair recombination process of singlet−singlet or triplet−triplet states may occurs generating different products and yields, even when bimolecular systems are taken into account.[42] Figure 1a shows that for the first 50 fs, the excitons remain very close to each other, which is an indication of a small interaction between them, consequence of the electron−electron interactions considered. From that

dx.doi.org/10.1021/jp4107926 | J. Phys. Chem. B 2014, 118, 5250−5257

instant on, the electric field strength becomes considerable and the interaction between the electrons and holes of both excitons is increased, which is easily verified by noting the spacing among the exciton at around 300 fs and the phonons produced through the lattice. These phonons are the direct manifestation of the excitons interaction causing the diffusive pattern presented by Figure 1a. These facts suggest that the electric field is fundamental to increase the interaction between the excitons toward the production of new species. Another important characteristic to observe is that the electric field plays the role of concentrating charge in the quasi-particles lattice distortion. Figure 1b presents the charge density time evolution. It is possible to note that before approximately 50 fs, when the electric field regime is too small, there is almost no charge concentration in the system. Immediately after this moment, a negative (blue) and a positive (red) concentration of charge arise in the chain as a consequence of a higher electric field action, in this case, 1.5 mV/Å. After a small transient time for the electric field response, the generated free charge carriers begin to move toward one another due to the opposite charges they possess. Before the collision between the charge carriers, two excited polarons (polaron-excitons) emerge from the exciton recombination process and their dynamics occurs as described by Stafström and co-workers.[33,34] At approximately 580 fs, when the collision takes place, one can see a transition structure that is momentarily self-trapped around the 100th site for about 200 fs. Thus, after the conditions for creating this transition structure is achieved, the electric field tends to destabilize such structure and to direct the system to the final state composed of a bipolaron-exciton with positive charge and a polaron-exciton that have negative charge. The polaron-exciton passes through the bipolaron-exciton in a process that yields the formation of a mixed state composed of charge carriers and excitons after the scattering. Also, the interaction between the hole-bipolaron (BP^+) and the electron-polaron (P^-) increases the production of phonons after the scattering, as showed in Figure 1a. For the simulations performed considering the electric field effects and Coulomb interactions, in the absence of the temperature, the results showed that for all electric field strengths smaller than 1.5 mV/Å the exciton recombination does not take place. In theses cases, only a separation between the excitons can be observed, in the same fashion as observed in Figure 1a. On the other hand, for electric field regimes greater than this critical value, the same products shown in Figure 1b are formed. A further increase in the electric field strength leads to a yield gain in the bipolaron and polaron formation, due to the fact that a larger electrons fraction is transferred among the energy levels of the excitons. This process provides, for example, a well-defined bipolaron with a faster response to the electric field action than the case for the critical electric field showed in Figure 1a,b.

A more realistic theoretical description is obtained by discussing the qualitative dynamical features of the recombination process between the singlet exciton pair considering the contribution of the temperature effects to this mechanism. Figure 1c,d depicted the second channel for the singlet−singlet exciton recombination reported in this work. For this case, the temperature regime is 150 K, the electric field strength is 1.5 mV/Å, and the Coulomb interaction is 0.2 eV. Figure 1c shows that, after about 50 fs, the adding up of thermal energy begins to become visible through the blurring of the figure. After about 90 fs, the lattice oscillations are of such amplitude that causes the direct generation of two free oppositely charged polaron-excitons. In this case, both particle maintain their integrity until the end of the simulation, as can be seen in Figure 1d. However, the disordered pattern on the order parameter, shown in Figure 1c, indicates that a reduction of stability of the polaron-excitons occurs caused by the large amplitude of the lattice vibration induced by the temperature. By analyzing the polaron-excitons trajectory in Figure 1c, one can readily note the influence temperature has over the quasi-particles by the damping of their movements. This behavior is attributed to the fact that the lattice vibration disturbs the system in such a level that the electric field is no longer able to give considerable velocity for the free charge carriers. Also, it was observed that, when the temperature effects are considered in the presence of electron−electron interactions and, most important, of an external electric field, the singlet−singlet exciton recombination in a high-density region leads directly to the formation of identical free charge carriers with opposite charges, i.e., an electron-polaron (P^-) and a hole-polaron (P^+) for all temperature regimes simulated. As discussed in the first channel, for the physical picture presented in Figure 1c,d (second channel), the electric field effects also play to role to produce free charge carriers with better yield than neutral excitations, although the final product is still a mixed state of free charge carriers and neutral excitons. In summary, the second channel depicts the most remarkable result from the simulations reported in this paper, suggesting that there may be an alternative route for creating an oppositely charged polaron pair when a reasonable relation between the density of excitons, electric field, and temperature is considered.

To elucidate the influence of the temperature and electric field effects on the dynamical process of singlet−singlet exciton recombination, the next natural step is the consideration of a system in which temperature effects and Coulomb interaction are taken into account in the absence of an external electric field. Figure 2 presents the remaining recombination channel

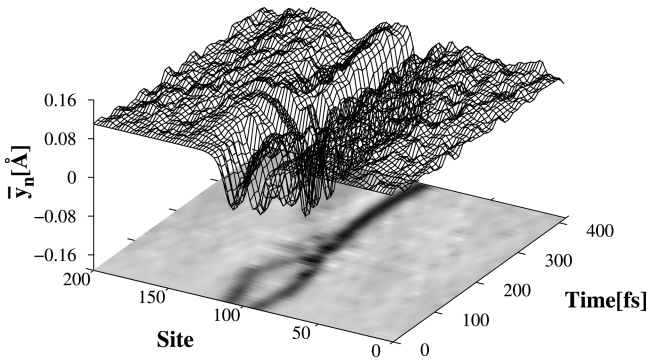

Figure 2. Bond-length order parameter time evolution that depicts the singlet biexcitonic state formation (channel 3) for T = 100 K, U = 0.2 eV, and E = 0.

reported in this work. The figure shows the bond length time evolution for a temperature regime of 100 K and electron−electron interactions strength of 0.2 eV. In this case, the wave functions of the two singlet excitons start to overlap strongly because the two excitons are positioned very close to each other at the beginning of the simulation. The random walk dynamics resultant from temperature fluctuations eventually causes the pair of excitons to be again close together at about 100 fs. Together with the temperature effects, the Coulomb interaction of the self-trapped state helps producing a singlet biexciton

dx.doi.org/10.1021/jp4107926 | J. Phys. Chem. B 2014, 118, 5250−5257

(SBE) deformation by transferring a fraction of the two electrons from a singlet exciton to the other one. The result of this process can be clearly seen observing the lattice deformation before and after the exciton pair recombination in Figure 2. The surface shows the motion of the lattice carbon sites resulting from the thermal oscillations that increases over time, which indicates that the thermalization process is not instantaneous. After 100 fs, it is possible to note that only one quasi-particle structure, which characterizes the singlet biexcitonnic state, remains in the lattice. This behavior was observed for all temperature regimes simulated here. Also, by observing the surface projection, shown at the bottom of Figure 2, one can see that the singlet biexcitonnic structure causes a greater lattice deformation than the conventional singlet exciton. This fact suggests that the biexciton is a more stable structure than the singlet exciton. Indeed, theoretical calculations have shown that the radiative decay process of a biexciton has a large transition dipole moments (8.8 e Å), in such a way that the biexciton state can decay into a singlet exciton sate by emitting one photon.[13] Furthermore, the resultant singlet exciton has also a large transition dipole momentum (5.5 e Å), which is of the same order of magnitude as that of the biexciton and the singlet exciton decay to the ground state emitting one photon. These results indicate that the above-discussed mechanism of Figure 3, leading to the

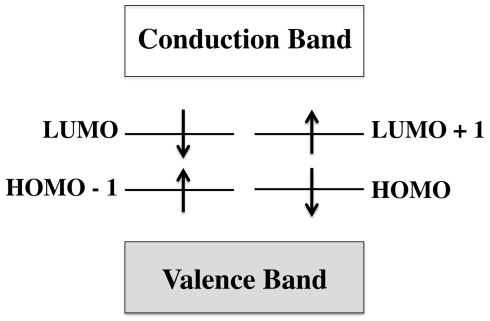

Figure 3. Illustration of the bandgap structure for a polymer chain containing a singlet exciton pair with antiparallel spin configuration.

biexciton formation, requires a more energetic situation than the initial configuration with a singlet-exciton pair for dissociating the biexciton. Also, this process limits the free charge carrier generation mechanism only in the biexciton dissociation at the donor−acceptor heterojunction interface, unlike the results reported in channel 2. Thus, it is possible to conclude that the temperature effects act on the system in a way to decrease the free charge carrier generation when a region with high-density of excitons is considered. On the other hand, the results reported in channels 1 and 2 indicate that the electric field effects are of fundamental importance and favors the free charge carrier formation.

The yields of the mixed state composed of free charge carriers and neutral excitations, is efficiently described by means of the occupation number time evolution. In this context, Figure 3 shows the schematic diagram of energy levels for a polymer chain containing a singlet exciton pair with antiparallel spin configuration. There are four levels inside the bandgap. The two left levels, HOMO−1 and LUMO, represent the electronic configuration for one of the singlet excitons present in the lattice, in which the upper and the lower ones are occupied by one electron with opposite spins. The right levels, HOMO and LUMO+1, represent an alternative route to create a singlet exciton structure, having antiparallel spin configuration with respect to the first one. Figure 4 shows the occupation number time evolution for channel 1 (Figure 4a), channel 2 (Figure 4b), and channel 3 (Figure 4c). In Figure 4a, after the transient period in which the occupation number oscillates due to the strong overlapping of singlet excitons, it is possible to

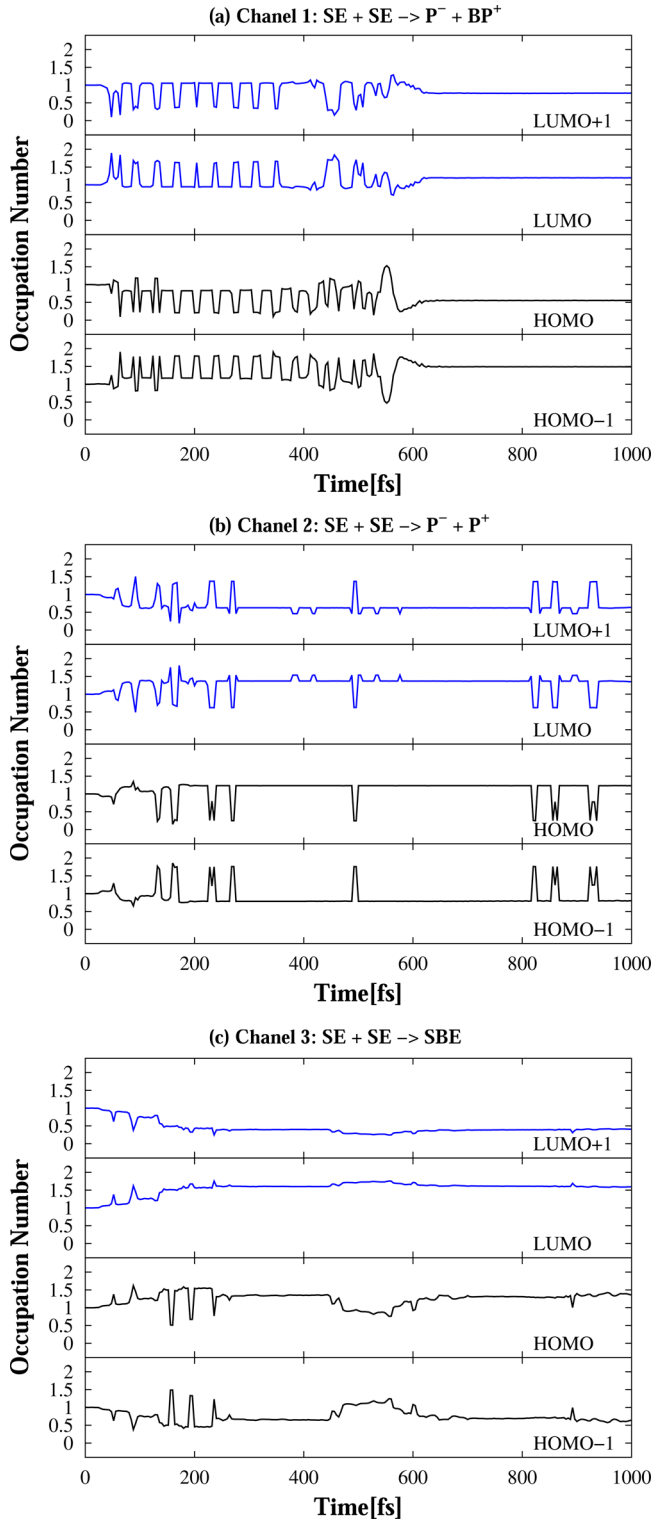

Figure 4. Occupation number time evolution for (a) channel 1, (b) channel 2, and (c) channel 3.

dx.doi.org/10.1021/jp4107926 | J. Phys. Chem. B 2014, 118, 5250−5257

note a considerable degree of symmetry between HOMO−1 and HOMO and also between LUMO and LUMO+1, which is an indication of an electron exchange between these levels. The electron exchange after approximately 580 fs between the levels represents the formation of a polaron-exciton structure (electron-polaron + singlet-exciton), being represented by the HOMO−1 level filled almost with two electrons and the LUMO that has one entire electron together with a quite small fraction of another electron. The bipolaron-exciton (hole-bipolaron + singlet-exciton) has the bandgap electronic configuration presented by the HOMO and LUMO+1 both occupied practically with one electron.

Figure 4b shows the occupation number time evolution for the case depicted in the channel 2, where two free polaron-excitons with opposite charge are created. By analyzing the occupation number itself, one can see that the final states are not covered by integer numbers, which is evidence of partial transfer. Moreover, in this case, the occupation numbers do not present the oscillating pattern with high frequency as shown Figure 4a. This fact can be attributed to the temperature influence on the system that gives random motion to the excitons decreasing significantly the overlap interaction between them. The HOMO−1 and the LUMO levels represent the negative polaron-exciton structure (electron-polaron + singlet exciton), whereas the HOMO and the LUMO+1 levels define the positive polaron-exciton (hole-polaron + singlet exciton). In this channel the polaron-excitons formed can be distinguished by observing the LUMO levels. The LUMO+1 level is occupied by a fraction of approximately 0.5 electron, forming the hole-polaron. On the other hand, the LUMO level is filled by 1.5 fraction of electrons, which generates the electron-polaron. Finally, Figure 4c depicts the occupation number time evolution for the physical picture where a biexciton is formed. Through this figure one can see that the final stage of the biexciton formation takes place at approximately 200 fs. At the end of the simulation, both levels are occupied by about half electron. Consequently, the HOMO and LUMO levels remain inside the energy gap and are filled by almost 1.5 electrons. Also, in this case the temperature acts on the system in a way to decrease the electron oscillation between the quasi-particle energy levels inside the bandgap.

The analysis of the time evolution of energy levels is recognized as one of the most suitable tools to describe the products generated after a recombination process between quasi-particles in conjugated polymers.[11,12,39,40] Figure 5 shows the energy level time evolution profile of the simulations that corresponds to the aforementioned channels: Figure 5a shows the energy level behavior for the channel 1 (SE + SE → BP^+ + P^-), Figure 5b presents the results for the channel 2 (SE + SE → P^+ + P^-), and Figure 5c for the last discussed channel (SE + SE → SBE). Concerning these three figures, the first result to consider is that the presence of an external electric is responsible for causing the degeneracy break in the energy levels inside the valence and conduction bands. This conclusion results from the fact that this degeneracy breaking is missing in Figure 5c, which was carried out in the absence of an external electric field. Studying Figure 5a shows the recombination process takes place at approximately 600 fs, forming two different new species when the resulting phonons are associated with the oscillation of the energy levels inside the bandgap. The signature of the hole-bipolaron (BP^+) formation is related to the presence of states deep inside the energy gap (blue lines) that represents its integrity. The red levels, which remain

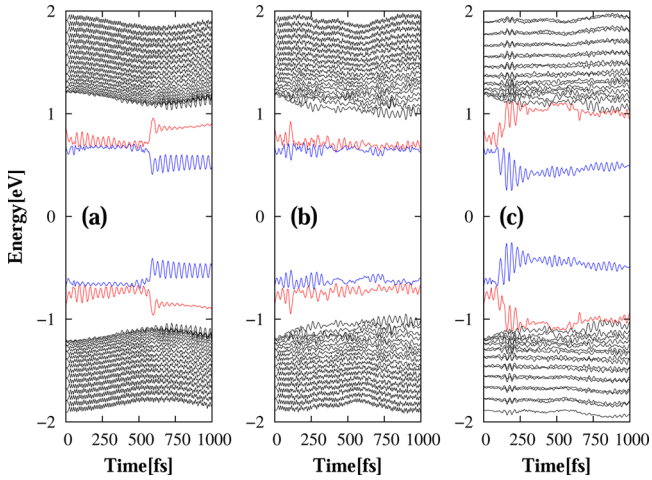

Figure 5. Energy levels time evolution for the (a) channel 1, SE + SE → BP^+ + P^-, (b) channel 2, SE + SE → P^+ + P^-, and (c) channel 3, SE + SE → SBE.

consistently inside the bandgap, represent the electron-polaron (P^-) formation and are closer of the valence and conduction band. In Figure 5b it is possible observe that the two oppositely charged polaron-excitons are formed directly after approximately 50 fs. Also, comparing the polaron-exciton energy levels inside the bandgap of Figure 5b with the red levels (that represents the polaron-exciton) in Figure 5a, one can see that the red levels in Figure 5a are closer to the valence and conduction band than all the other levels present inside the bandgap of Figure 5b. This fact suggests that the polaron-exciton formed in the recombination process described for channel 1 has a yield of polaron formation greater than excitons. On the other hand, for the recombination products reported in channel 2, the energy levels behavior indicates that the mixed state composed of polarons and neutral excitations formed after the recombination process present a higher yield in the excitons formation. Once the simulations presented in the channel 1 were performed in the absence of the temperature, the results reported in channels 2 and 3 are evidence that the thermal effects play the role of producing neutral excitations after the exciton recombination process. The singlet biexcitonic state generation of Figure 2 corresponds to features that can be exactly inferred by analyzing the red energy levels that returns to the valence and conduction band, as shown in Figure 5c, thus leading to the vanishing of one singlet exciton. Furthermore, in Figure 5c, at about 100 fs, it is possible to note that the recombination takes place and blue levels, which represent the singlet biexciton, remain inside the energy gap until the end of the simulation. It is important to remark that temperature effects increase the oscillation pattern presented by the energy levels due to the presence of phonons with higher energies. However, these effects do not act in a way to break the degeneracy in the levels inside the valence and conduction band.

SUMMARY AND CONCLUSIONS

A modified version of the SSH model to include an external electric field, the Brazovskii−Kirova symmetry breaking term, one-site and nearest-neighbor electron−electron Coulomb interactions, and temperature is presented to investigate the effects of these properties over the recombination process of a singlet exciton pair in cis-symmetry conducting polymers

dx.doi.org/10.1021/jp4107926 | J. Phys. Chem. B 2014, 118, 5250−5257

chains. Using a nonadiabatic evolution method, within a one-dimensional tight-binding model, the excitons are positioned very close to each other in a way to mimic a high-density region in monomolecular systems. Considering this physical picture, one finds that there are three possible channels resulting from singlet−singlet exciton recombination: (1) formation of an excited negative polaron and an excited positive bipolaron, in the absence of temperature, when the effects over the system of an external electric field and Coulomb interaction are taken into account; (2) generation of two free and excited oppositely charged polarons, when the thermal effects are considered together with an moderate external electric field regime and electron−electron interactions; (3) creation of a biexciton in the absence of an external electric field. These results suggest that temperature effects act on the system in a way to decrease the free charge carrier formation when a region with high-density of excitons is considered, whereas electric field effects are of fundamental importance and favors the free charge carrier generation. Moreover, the second channel represents the principal result from the simulations reported in this work, which suggests that there may be an alternative route to creating free charge carriers (hole-polaron and electron-polaron) when a appropriate relation between the density of excitons, electric field, and temperature is considered.

AUTHOR INFORMATION

Corresponding Authors

*L. A. Ribeiro Junior: e-mail, ribeirojr@fis.unb.br.

*G. M. e Silva: e-mail, magela@fis.unb.br.

Notes

The authors declare no competing financial interest.

ACKNOWLEDGMENTS

The gratefully acknowledge the financial support from the Brazilian Research Councils CAPES, CNPq, and FINATEC.

REFERENCES

(1) Menke, S. M.; Luhman, W. A.; Holmes, R. J. Tailored Exciton Diffusion in Organic Photovoltaic Cells for Enhanced Power Conversion Efficiency. *Nat. Mater.* **2013**, *12*, 152−157.

(2) Jailaubekov, A. E.; Willard, A. P.; Tritsch, J. R.; Chan, W.-L.; Sai, N.; Gearba, R.; Kaake, L. G.; Williams, K. J.; Leung, K.; Rossk, P. J.; Zhu, X.-Y. Hot Charge-Transfer Excitons Set the Time Limit for Charge Separation at Donor/Acceptor interfaces in organic photovoltaics. *Nat. Mater.* **2013**, *12*, 66−73.

(3) Grancini, G.; Maiuri, M.; Fazzi, D.; Petrozza, A.; Egelhaaf, H.-J.; Brida, D.; Cerullo, G.; Lanzani, G. Hot Exciton Dissociation in Polymer Solar Cells. *Nat. Mater.* **2013**, *12*, 29−33.

(4) Yang, Q.; Liu, Y.; Pan, C.; Chen, J.; Wen, X.; Wang, Z. L. Largely Enhanced Efficiency in ZnO Nanowire/p-Polymer Hybridized Inorganic/Organic Ultraviolet Light-Emitting Diode by Piezo-Phototronic Effect. *Nano Lett.* **2013**, *13*, 607−613.

(5) Tang, S.; Pan, J.; Buchholz, H. A.; Edman, L. White Light from a Single-Emitter Light-Emitting Electrochemical Cell. *J. Am. Chem. Soc.* **2013**, *13*, 3647−3652.

(6) Zuniga, C. A.; Abdallah, J.; Haske, W.; Zhang, Y.; Coropceanu, I.; Barlow, S.; Kippelen, B.; Marder, S. R. Crosslinking Using Rapid Thermal Processing for the Fabrication of Efficient Solution-Processed Phosphorescent Organic Light-Emitting Diodes. *Adv. Mater.* **2013**, *25*, 1793−1744.

(7) Barford, W. Excitons in Conjugated Polymers: A Tale of Two Particles. *J. Phys. Chem. A* **2013**, *25*, 2665−2671.

(8) Barford, W. Theory of Singlet Exciton Yield in Light-Emitting Polymers. *Phys. Rev. B* **2004**, *70*, 205204−205212.

(9) Brazovskii, S.; Kirova, N. Physical Theory of Excitons in Conducting Polymers. *Chem. Soc. Rev.* **2010**, *39*, 2453−2465.

(10) Meng, Y.; Liu, X. J.; Di, B.; An, Z. Recombination of Polaron and Exciton in Conjugated Polymers. *J. Chem. Phys.* **2009**, *131*, 244502−5.

(11) Sun, Z.; Liu, D.; Stafström, S.; An, Z. Scattering Process Between Polaron and Exciton in Conjugated Polymers. *J. Chem. Phys.* **2011**, *134*, 044906−044911.

(12) Sun, Z.; Li, Y.; Li, D. S.; An, Z.; Xie, S. Scattering Process Between Bipolaron and Exciton in Conjugated Polymers. *Phys. Rev. B* **2009**, *134*, 201310(R).

(13) Di, B.; Meng, Y.; Wang, Y. D.; Liu, X. J.; An, Z. Formation and Evolution Dynamics of Bipolarons in Conjugated Polymers. *J. Chem. Phys. B* **2011**, *115*, 964−971.

(14) Di, B.; Meng, Y.; Wang, Y. D.; Liu, X. J.; An, Z. Electroluminescence Enhancement in Polymer Light-Emitting Diodes through Inelastic Scattering of Oppositely Charged Bipolarons. *J. Chem. Phys. B* **2011**, *115*, 9339−9344.

(15) Stafström, S. Electron Localization and the Transition from Adiabatic to Nonadiabatic Charge Transport in Organic Conductors. *Chem. Soc. Rev.* **2010**, *39*, 2484−2499.

(16) Ribeiro, L. A.; Neto, P. H. O.; da Cunha, W. F.; Roncaratti, L. F.; Gargano, R.; da Silva Filho, D. A.; e Silva, G. M. Exciton Dissociation and Charge Carrier Recombination Processes in Organic Semiconductors. *J. Chem. Phys.* **2011**, *135*, 224901−224906.

(17) Neto, P. H. O.; da Cunha, W. F.; Roncaratti, L. F.; Gargano, R.; e Silva, G. M. Thermal Effects on Photogeneration of Free Carriers in Organic Conductors. *Chem. Phys. Lett.* **2010**, *493*, 283−287.

(18) Su, W. P.; Schrieffer, J. R.; Heeger, A. J. Solitons in Polyacetylene. *Phys. Rev. Lett.* **1979**, *42*, 1698−1701.

(19) Su, W. P.; Schrieffer, J. R.; Heeger, A. J. Solitons Excitations in Polyeacetylene. *Phys. Rev. B* **1980**, *22*, 2099−2111.

(20) Pinheiro, C. S.; e Silva, G. M. Use of Polarons and Bipolarons in Logical Switches Based on Conjugated Polymers. *Phys. Rev. B* **2002**, *65*, 094304−5.

(21) Yu, Z. G.; Wu, M. W.; Rao, X. S.; Bishop, A. R. Excitons in Two Coupled Conjugated Polymer Chains. *J. Phys. Condes. Matter* **1996**, *8*, 8847−8857.

(22) Leng, J. M.; Jeglinski, S.; Wei, X.; Benner, R. E.; Vardeny, Z. V.; Guo, F.; Mazumdar, S. Optical Probes of Excited States in Poly(p-Phenylenevinylene). *Phys. Rev. Lett.* **1994**, *72*, 156−159.

(23) Hsu, J. W. P.; Yan, M.; Jedju, T. M.; Rothberg, L. J.; Hsieh, B. R. Assignment of the Picosecond Photoinduced Absorption in Phenylene Vinylene Polymers. *Phys. Rev. B* **1994**, *49*, 712(R).

(24) Chandross, M.; Mazumdar, S.; Jeglinski, S.; Wei, X.; Vardeny, Z. V.; Kwock, E. W.; Miller, T. M. Excitons in Poly(para-Phenylenevinylene). *Phys. Rev. B* **1994**, *50*, 14702(R).

(25) Yu, Z. G.; Fu, R. T.; Wu, C. Q.; Sun, X.; Nasu, K. Excitons, Biexcitons, and the Band Gap in Poly(P-Phenylenevinylene). *Phys. Rev. B* **1995**, *52*, 4849−4854.

(26) Guo, F.; Chandross, M.; Mazumdar, S. Stable Biexcitons in Conjugated Polymers. *Phys. Rev. Lett.* **1995**, *74*, 2086−2089.

(27) Soos, Z. G.; Ramasesha, S.; Galvao, D. S.; Etemad, S. Excitation and Relaxation Energies of Trans-Stilbene: Confined Singlet, Triplet, and Charged Bipolarons. *Phys. Rev. B* **1993**, *47*, 1742−1753.

(28) Ramasesha, S.; Pati, S. K.; Krishnamurthy, H. R.; Shuai, Z.; Brédas, J. L. Symmetrized Density-Matrix Renormalization-Group Method for Excited States of Hubbard Models. *Phys. Rev. B* **1996**, *54*, 7598−7600.

(29) Shuai, Z.; Brédas, J. L.; Pati, S. K.; Ramasesha, S. Exciton Binding Energy in the Strong Correlation Limit of Conjugated Chains. *Phys. Rev. B* **1998**, *58*, 15329−15331.

(30) Neto, P. H. O.; da Cunha, W. F.; Teixeira, J. F.; Gargano, R.; e Silva, G. M. Electron-Lattice Coupling in Armchair Graphene Nanoribbons. *J. Phys. Chem. Lett.* **2012**, *3*, 3039−3042.

(31) Ribeiro, L. A.; da Cunha, W. F.; Neto, P. H. O.; Gargano, R.; e Silva, G. M. Predicting the Equilibrium Structure of Organic Semiconductors With Genetic Algorithms. *Chem. Phys. Lett.* **2013**, *555*, 168−172.

(32) Ribeiro, L. A.; da Cunha, W. F.; Neto, P. H. O.; e Silva, G. M. Dynamics of Photogenerated Polaron-Excitons in Organic Semiconductors. *Phys. Proc.* **2012**, *28*, 112−116.
(33) Johansson, A.; Stafström, S. Polaron Dynamics in a System of Coupled Conjugated Polymer Chains. *Phys. Rev. Lett.* **2001**, *86*, 3602−3605.
(34) Johansson, A.; Stafström, S. Nonadiabatic Simulations of Polaron Dynamics. *Phys. Rev. B* **2004**, *69*, 235205−7.
(35) An, Z.; Wu, C. Q.; Sun, X. Dynamics of Photogenerated Polarons in Conjugated Polymers. *Phys. Rev. Lett.* **2004**, *93*, 216407−4.
(36) e Silva, G. M.; Terai, A. Dynamics of Solitons in Polyacetylene With Interchain Coupling. *Phys. Rev. B* **1993**, *47*, 12568−12577.
(37) e Silva, G. M. Electric-Field Effects on the Competition Between Polarons and Bipolarons in Conjugated Polymers. *Phys. Rev. B* **2000**, *61*, 10777−10781.
(38) Lima, M. P.; e Silva, G. M. Dynamical Evolution of Polaron to Bipolaron in Conjugated Polymers. *Phys. Rev. B* **2006**, *74*, 224303−6.
(39) Ribeiro, L. A.; da Cunha, W. F.; Neto, P. H. O.; Gargano, R.; e Silva, G. M. Impurity Effects on Polaron-Exciton Formation in Conjugated Polymers. *J. Chem. Phys.* **2013**, *139*, 174903−114.
(40) Ribeiro, L. A.; da Cunha, W. F.; Neto, P. H. O.; Gargano, R.; e Silva, G. M. Dynamical Study of Impurity Effects on Bipolaron-Bipolaron and Bipolaron-Polaron Scattering in Conjugated Polymers. *J. Phys. Chem. B* **2013**, *117*, 11801−11811.
(41) Ribeiro, L. A.; da Cunha, W. F.; Neto, P. H. O.; Gargano, R.; e Silva, G. M. Impurity Effects and Temperature Influence on the Exciton Dissociation Dynamics in Conjugated Polymers. *Chem. Phys. Lett.* **2013**, *580*, 108−114.
(42) Ribeiro, L. A.; da Cunha, W. F.; Neto, P. H. O.; Gargano, R.; e Silva, G. M. Effects of Temperature and Electric Field Induced Phase Transitions on the Dynamics of Polarons and Bipolarons. *New J. Chem.* **2013**, *37*, 2829−2836.
(43) Sun, Z.; Stafstöm, S. Dynamics of Exciton Dissociation in Donor-Acceptor Polymer Heterojunctions. *J. Chem. Phys.* **2013**, *138*, 164905−8.
(44) Roncaratti, L. F.; Gargano, R.; de Oliveira Neto, P. H.; da Cunha, W. F.; da Silva Filho, D. A.; e Silva, G. M. Temperature-Induced Oscillating Electric Dipole in Conjugated Systems. *Chem. Phys. Lett.* **2012**, *593*, 214−217.
(45) Roncaratti, L. F.; Gargano, R.; e Silva, G. M. Theoretical Temperature Dependence of the Charge-Carrier Mobility in Semiconducting Polymers. *J. Phys. Chem. A* **2009**, *113*, 14591−14594.
(46) Sun, Z.; Stafström, S. Spin-Dependent Polaron Recombination in Conjugated Polymers. *J. Chem. Phys.* **2012**, *136*, 244901−5.